

Chiral 2π -exchange NN-potentials: Two-loop contributions

N. Kaiser

Physik Department T39, Technische Universität München, D-85747 Garching, Germany

Abstract

We calculate in heavy baryon chiral perturbation theory the local NN-potentials generated by the two-pion exchange diagrams at two-loop order. We give explicit expressions for the mass-spectra (or imaginary parts) of the corresponding isoscalar and isovector central, spin-spin and tensor NN-amplitudes. We find from two-loop two-pion exchange a sizeable isoscalar central repulsion which amounts to 62.3 MeV at $r = 1.0$ fm. There is a similarly strong isovector central attraction which however originates mainly from the third order low energy constants \bar{d}_j entering the chiral πN -scattering amplitude. We also evaluate the one-loop 2π -exchange diagram with two second order chiral $\pi\pi NN$ -vertices proportional to the low energy constants $c_{1,2,3,4}$ as well as the first relativistic $1/M$ -correction to the 2π -exchange diagrams with one such vertex. The diagrammatic results presented here are relevant components of the chiral NN-potential at next-to-next-to-next-to-leading order.

PACS: 12.20.Ds, 12.38.Bx, 12.39.Fe, 13.75.Cs.

Over the past years effective field theory methods have been successfully applied to the two-nucleon system at low and intermediate energies [1, 2, 3, 4, 5, 6]. The idea of constructing the NN-potential from effective field theory was put forward by Weinberg [1] and this was first taken up by van Kolck and collaborators [2] who used "old-fashioned" time-ordered perturbation theory. Later, the systematic method of unitary transformations was employed by Epelbaum, Glöckle and Meißner [4] to construct an energy-independent NN-potential from the effective chiral pion-nucleon Lagrangian at next-to-leading order. Based on one- and two-pion exchange and nine adjustable NN-contact interactions which contribute only to S- and P-waves a good description of the deuteron properties as well as the NN phase-shifts and mixing angles below $T_{lab} = 300$ MeV was found in that framework [4]. Also recently, the elastic proton-proton scattering data base below 350 MeV laboratory kinetic energy (consisting of 1951 data points) has been analyzed in terms of 1π -exchange and chiral 2π -exchange at next-to-next-to-leading order in ref.[7]. The resulting good $\chi^2/dof \leq 1$ constitutes a convincing proof for the presence of the chiral 2π -exchange in the long-range proton-proton strong interaction. It was concluded in ref.[7] that 1π -exchange together with chiral 2π -exchange gives a very good NN-force at least as far inwards as $r = 1.4$ fm internucleon distance. All shorter range components of the NN-interaction have been effectively parametrized in ref.[7] by 23 boundary condition parameters.

At present, there is much interest in extending the calculations of the two-nucleon system [8] (and also the analysis of the NN-data base) to one higher order in the chiral expansion. This requires the full knowledge of the next-to-next-to-next-to-leading order (N^3LO) chiral NN-potential. In momentum space this corresponds to terms in the NN T-matrix which are of fourth order in small external momenta and the pion mass, denoted generically by $\mathcal{O}(Q^4)$. In particular, all two-loop diagrams of the process $NN \rightarrow NN$ with leading order vertices contribute at that order, $\mathcal{O}(Q^4)$. In three recent publications [9] we have calculated completely the static NN-potentials generated by the (two-loop) 3π -exchange diagrams with all possible interaction vertices taken from the leading-order effective chiral πN -Lagrangian. In these works we have evaluated the mass-spectra or imaginary parts from which one can also easily reconstruct the momentum space NN-amplitudes in the form of a subtracted dispersion relation. The appearing subtraction constants can be absorbed in the strengths of some local NN-contact interactions

which will be treated as adjustable parameters in a fit to NN-phase shifts etc. The purpose of this work is to present analogous results for the two-loop contributions to the chiral 2π -exchange which also belong to the chiral NN-potential at order $\mathcal{O}(Q^4)$. Furthermore, we evaluate several new contributions at the same order $\mathcal{O}(Q^4)$. These are the one-loop 2π -exchange diagram with two second order chiral $\pi\pi NN$ -vertices proportional to the low energy constants $c_{1,2,3,4}$ and the first relativistic $1/M$ -corrections to the 2π -exchange diagrams with one such vertex proportional to $c_{1,2,3,4}$.

Let us first give some basic definitions in order to fix our notation. In the static limit and considering only irreducible diagrams the on-shell NN T-matrix takes the following form

$$\begin{aligned} \mathcal{T}_{NN} = & V_C(q) + V_S(q) \vec{\sigma}_1 \cdot \vec{\sigma}_2 + V_T(q) \vec{\sigma}_1 \cdot \vec{q} \vec{\sigma}_2 \cdot \vec{q} \\ & + [W_C(q) + W_S(q) \vec{\sigma}_1 \cdot \vec{\sigma}_2 + W_T(q) \vec{\sigma}_1 \cdot \vec{q} \vec{\sigma}_2 \cdot \vec{q}] \vec{\tau}_1 \cdot \vec{\tau}_2, \end{aligned} \quad (1)$$

where $q = |\vec{q}|$ denotes the momentum transfer between the initial and final-state nucleon. The subscripts C, S and T refer to the central, spin-spin and tensor components, each of which occurs in an isoscalar ($V_{C,S,T}$) and an isovector version ($W_{C,S,T}$). As indicated, the (real) NN-amplitudes $V_C(q), \dots, W_T(q)$ depend only on the momentum transfer q in the static limit $M \rightarrow \infty$, where M denotes the nucleon mass. We are interested here only in non-polynomial or finite range terms. For this purpose it is sufficient to calculate the imaginary parts of the NN-amplitudes, $\text{Im} V_{C,S,T}(i\mu)$ and $\text{Im} W_{C,S,T}(i\mu)$, which result from analytical continuation to time-like momentum transfer $q = i\mu - 0^+$ with $\mu \geq 2m_\pi$. These imaginary parts are also the mass-spectra entering a representation of the local coordinate-space potentials in the form of a continuous superposition of Yukawa-functions,

$$\tilde{V}_C(r) = -\frac{1}{2\pi^2 r} \int_{2m_\pi}^{\infty} d\mu \mu e^{-\mu r} \text{Im} V_C(i\mu), \quad (2)$$

$$\tilde{V}_S(r) = \frac{1}{6\pi^2 r} \int_{2m_\pi}^{\infty} d\mu \mu e^{-\mu r} [\mu^2 \text{Im} V_T(i\mu) - 3 \text{Im} V_S(i\mu)], \quad (3)$$

$$\tilde{V}_T(r) = \frac{1}{6\pi^2 r^3} \int_{2m_\pi}^{\infty} d\mu \mu e^{-\mu r} (3 + 3\mu r + \mu^2 r^2) \text{Im} V_T(i\mu). \quad (4)$$

The isoscalar central, spin-spin and tensor potentials, denoted here by $\tilde{V}_{C,S,T}(r)$, are as usual those ones which are accompanied by the operators 1 , $\vec{\sigma}_1 \cdot \vec{\sigma}_2$ and $3\vec{\sigma}_1 \cdot \hat{r} \vec{\sigma}_2 \cdot \hat{r} - \vec{\sigma}_1 \cdot \vec{\sigma}_2$, respectively. For the isovector potentials $\tilde{W}_{C,S,T}(r)$ a completely analogous representation holds, of course.

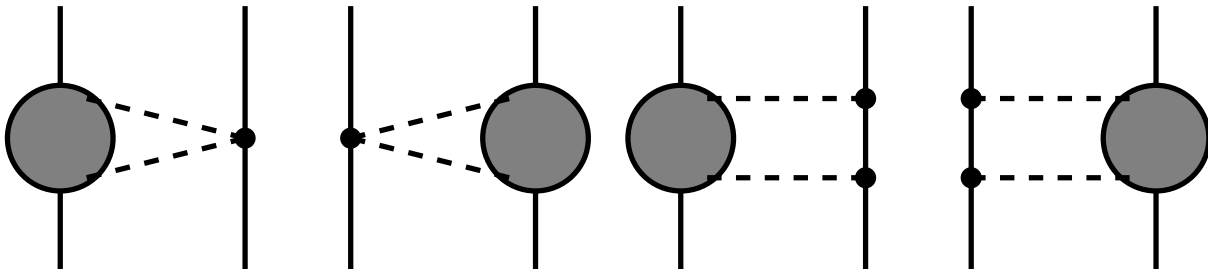


Fig.1: 2π -exchange diagrams at two-loop order. The grey disc symbolizes all one-loop diagrams of elastic πN -scattering. The combinatoric factor of the first two diagrams is $1/2$. Diagrams for which the role of both nucleons is interchanged lead to the same NN-potential.

The two-loop 2π -exchange diagrams are symbolically represented in Fig.1. The grey disc should be interpreted such that it includes all one-loop diagrams of elastic πN -scattering. The imaginary parts entering eqs.(2,3,4) can be calculated from these 2π -exchange diagrams as integrals of the $\bar{N}N \rightarrow 2\pi \rightarrow \bar{N}N$ transition amplitudes over the Lorentz-invariant 2π -phase

space making use of the Cutkosky cutting rule. In the present case these transition amplitudes are products of tree-level πN -amplitudes and one-loop πN -amplitudes. The pertinent 2π -phase space integral is most conveniently performed in the $\pi\pi$ center-of-mass frame where it becomes proportional to a simple angular integral $\int_{-1}^1 dx$. In the center-of-mass frame the on-shell pion four-momenta read $k_{1,2}^\nu = (\mu/2, \pm \vec{k})$ and as explained in ref.[9] the four-momenta of the external nucleons can be chosen as $P_{1,2}^\nu = (\pm\mu/2, p\vec{v})$ with \vec{v} a real unit vector and $p = \sqrt{\mu^2/4 - M^2} = iM + \mathcal{O}(M^{-1})$ in the heavy nucleon limit. As an extensive check on these techniques we have recalculated the imaginary parts of the one-loop 2π -exchange diagrams (considering graphs with no, single and double Δ -excitations, etc.) and we reproduced indeed exactly the results of refs.[5, 6] in a rather short calculation.

Let us now turn to the results for the 2π -exchange at two-loop order. From the last two diagrams in Fig. 1 we obtain the following imaginary part for the isoscalar central NN-amplitude,

$$\text{Im } V_C(i\mu) = \frac{3g_A^4(\mu^2 - 2m_\pi^2)}{\pi\mu(4f_\pi)^6} \left\{ (m_\pi^2 - 2\mu^2) \left[2m_\pi + \frac{2m_\pi^2 - \mu^2}{2\mu} \ln \frac{\mu + 2m_\pi}{\mu - 2m_\pi} \right] + 4g_A^2 m_\pi (2m_\pi^2 - \mu^2) \right\}. \quad (5)$$

Note that the expression in the curly bracket of eq.(5) is proportional to the isospin-even non-spin-flip one-loop πN -amplitude $\text{Re } g_{loop}^+(0, \mu^2)$ (see appendix A in ref.[10]). Modulo the last term proportional to g_A^2 this is precisely the result of the so-called correlated 2π -exchange given in section 4 of ref.[6]. Of very similar structure is the imaginary part of the isovector spin-spin (and tensor) NN-amplitude,

$$\text{Im } W_S(i\mu) = \mu^2 \text{Im } W_T(i\mu) = \frac{g_A^4(\mu^2 - 4m_\pi^2)}{\pi(4f_\pi)^6} \left\{ \left(m_\pi^2 - \frac{\mu^2}{4} \right) \ln \frac{\mu + 2m_\pi}{\mu - 2m_\pi} + (1 + 2g_A^2)\mu m_\pi \right\}. \quad (6)$$

Again, the expression in the curly bracket of eq.(6) is proportional to the isospin-odd spin-flip one-loop πN -amplitude $\text{Re } h_{loop}^-(0, \mu^2)$ [10]. Besides the last g_A^2 -term, eq.(6) agrees with result of correlated 2π -exchange given in ref.[6]. Next, we come to the imaginary parts of the isoscalar spin-spin and tensor NN-amplitudes. We obtain for them the following representation,

$$\begin{aligned} \text{Im } V_S(i\mu) = \mu^2 \text{Im } V_T(i\mu) &= \frac{2g_A^6\mu k^3}{(8\pi f_\pi^2)^3} \int_0^1 dx (1-x^2) \left\{ \frac{48\pi^2 f_\pi^2}{g_A^4} (d_{14}^r(\lambda) - d_{15}^r(\lambda)) - \ln \frac{m_\pi}{\lambda} \right. \\ &\quad \left. - \frac{1}{6} + \frac{m_\pi^2}{k^2 x^2} - \left(1 + \frac{m_\pi^2}{k^2 x^2} \right)^{3/2} \ln \frac{kx + \sqrt{m_\pi^2 + k^2 x^2}}{m_\pi} \right\}, \quad (7) \end{aligned}$$

with $k = \sqrt{\mu^2/4 - m_\pi^2}$ the pion center-of-mass momentum. Modulo the low-energy constant $d_{14}^r(\lambda) - d_{15}^r(\lambda)$ introduced in ref.[11] the expression in the curly bracket of eq.(7) is proportional to the isospin-even spin-flip one-loop πN -amplitude $\text{Re } [h_{loop}^+(\omega, \mu^2)/\omega]$ evaluated at $\omega = ikx$. All four diagrams in Fig. 1 contribute to the isovector central NN-amplitude $W_C(q)$ and we find for its imaginary part the following representation,

$$\begin{aligned} \text{Im } W_C(i\mu) &= \frac{2k}{3\mu(8\pi f_\pi^2)^3} \int_0^1 dx \left[g_A^2(2m_\pi^2 - \mu^2) + 2(g_A^2 - 1)k^2 x^2 \right] \left\{ 3k^2 x^2 \left(2 \ln \frac{m_\pi}{\lambda} - 1 \right) \right. \\ &\quad + 6kx \sqrt{m_\pi^2 + k^2 x^2} \ln \frac{kx + \sqrt{m_\pi^2 + k^2 x^2}}{m_\pi} + g_A^4(\mu^2 - 2k^2 x^2 - 2m_\pi^2) \\ &\quad \times \left[\frac{5}{6} - \ln \frac{m_\pi}{\lambda} + \frac{m_\pi^2}{k^2 x^2} - \left(1 + \frac{m_\pi^2}{k^2 x^2} \right)^{3/2} \ln \frac{kx + \sqrt{m_\pi^2 + k^2 x^2}}{m_\pi} \right] \\ &\quad + \left[4m_\pi^2(1 + 2g_A^2) - \mu^2(1 + 5g_A^2) \right] \frac{k}{\mu} \ln \frac{\mu + 2k}{2m_\pi} \\ &\quad - \frac{\mu^2}{2}(1 + 5g_A^2) \ln \frac{m_\pi}{\lambda} + \frac{\mu^2}{12}(5 + 13g_A^2) - 2m_\pi^2(1 + 2g_A^2) \\ &\quad \left. + 96\pi^2 f_\pi^2 \left[(2m_\pi^2 - \mu^2)(d_1^r(\lambda) + d_2^r(\lambda)) - 2k^2 x^2 d_3^r(\lambda) + 4m_\pi^2 d_5^r(\lambda) \right] \right\}. \quad (8) \end{aligned}$$

Again, modulo the low energy constants $d_j^r(\lambda)$ the expression in the curly bracket of eq.(8) is proportional to the isospin-odd non-spin-flip one-loop πN -amplitude $\text{Re}[g_{\text{loop}}^-(\omega, \mu^2)/\omega]$ evaluated at $\omega = ikx$. Furthermore, when restricting the second factor in eq.(8) to the terms in fourth and fifth line one recovers the result of correlated 2π -exchange given in section 4 of ref.[6]. The last line in eq.(8) gives the contribution of the third order low energy constants $d_{1,2,3,5}^r(\lambda)$ introduced in ref.[11]. Such counterterms are necessary in order to absorb the divergences generated by the one-loop graphs of elastic πN -scattering. In fact, the chiral logarithms $\ln(m_\pi/\lambda)$ and the scale dependent low energy constants $d_j^r(\lambda)$ in eqs.(7,8) combine to the (scale independent) barred quantities \bar{d}_j defined in ref.[11], or equivalently $\bar{d}_j = d_j^r(m_\pi)$. This completes the presentation of analytical results for the two-loop 2π -exchange NN-interaction. Modulo polynomials the momentum space NN-amplitudes $V_C(q), \dots, W_T(q)$ can be obtained in the form of a subtracted dispersion relation

$$V_{C,S}(q) = -\frac{2q^6}{\pi} \int_{2m_\pi}^{\infty} d\mu \frac{\text{Im} V_{C,S}(i\mu)}{\mu^5(\mu^2 + q^2)}, \quad V_T(q) = \frac{2q^4}{\pi} \int_{2m_\pi}^{\infty} d\mu \frac{\text{Im} V_T(i\mu)}{\mu^3(\mu^2 + q^2)}, \quad (9)$$

For the isovector amplitudes $W_{C,S,T}(q)$ a completely analogous dispersion relation representation holds, of course.

r [fm]	0.8	0.9	1.0	1.1	1.2	1.3	1.4	1.5	1.6
\tilde{V}_C [MeV]	249.6	120.3	62.28	34.18	19.67	11.77	7.29	4.64	3.03
\tilde{W}_S [MeV]	-27.80	-13.39	-6.93	-3.79	-2.18	-1.30	-0.803	-0.510	-0.331
\tilde{W}_T [MeV]	26.29	12.52	6.40	3.47	1.97	1.16	0.709	0.445	0.286
\tilde{V}_S [MeV]	166.9	71.07	32.96	16.36	8.59	4.73	2.71	1.60	0.977
\tilde{V}_T [MeV]	-140.0	-59.68	-27.49	-13.55	-7.07	-3.86	-2.19	-1.29	-0.780
\tilde{W}_C [MeV]	-503.6	-211.4	-96.81	-47.54	-24.73	-13.49	-7.67	-4.51	-2.74

Tab.1: Numerical values of the local NN-potentials generated by two-loop chiral 2π -exchange versus the nucleon distance r . The units of these potentials are MeV.

In Table 1, we present numerical values for the coordinate space potentials generated by chiral 2π -exchange at two-loop order inserting eqs.(5,6,7,8) into eqs.(2,3,4). We use the parameters $f_\pi = 92.4$ MeV, $m_\pi = 138$ MeV (average pion mass) and $g_A = 1.3$. Via the Goldberger-Treiman relation this corresponds to a strong πNN -coupling constant of $g_{\pi N} = g_A M / f_\pi = 13.2$ which is in agreement with present empirical determinations of $g_{\pi N}$ from πN -dispersion relation analyses [12]. For the third order low energy constants \bar{d}_j we use the average values of three fits to πN -phase shift solutions given in ref.[11]: $\bar{d}_1 + \bar{d}_2 = 3.0$ GeV⁻², $\bar{d}_3 = -3.0$ GeV⁻², $\bar{d}_5 = 0.1$ GeV⁻², $\bar{d}_{14} - \bar{d}_{15} = -5.7$ GeV⁻². One observes from Table 1 that the isoscalar central potential $\tilde{V}_C(r)$ generated by two-loop 2π -exchange is sizeable and repulsive. This repulsive potential is almost a factor 100 larger than the one from the so-called correlated 2π -exchange investigated in section 4 of ref.[6]. The origin of this strong enhancement is the additional and obviously dominant g_A^2 -term in the curly bracket of eq.(5) which stems from all those two-loop diagrams which were not considered in ref.[6]. Similar features hold for the attractive isovector spin-spin and the repulsive isovector tensor potentials $\tilde{W}_{S,T}(r)$ which are however typically a factor 10 smaller than isoscalar central potential $\tilde{V}_C(r)$. At first sight, the attractive isovector central potential $\tilde{W}_C(r)$ from two-loop 2π -exchange seems to be even larger in magnitude. However, in this case the effect comes mainly from the low energy constants \bar{d}_j . For example, if one omits the $d_j^r(\lambda)$ in eq.(8) and sets the scale $\lambda = m_\omega = 782$ MeV in the chiral logarithm $\ln(m_\pi/\lambda)$ the isoscalar central potential $\tilde{W}_C(r)$ gets reduced by more than one order of magnitude. The same phenomenon is observed for the isoscalar spin-spin and tensor potentials $\tilde{V}_{S,T}(r)$ which is also dominated by the contribution from the low-energy constant $\bar{d}_{14} - \bar{d}_{15}$. In the light of these findings one can expect that the

effect of including the two-loop 2π -exchange in NN-phase shift calculations is not just a small correction. Of course, a firm conclusion about the size of such corrections can only be drawn from the complete $N^3\text{LO}$ chiral NN-potential.

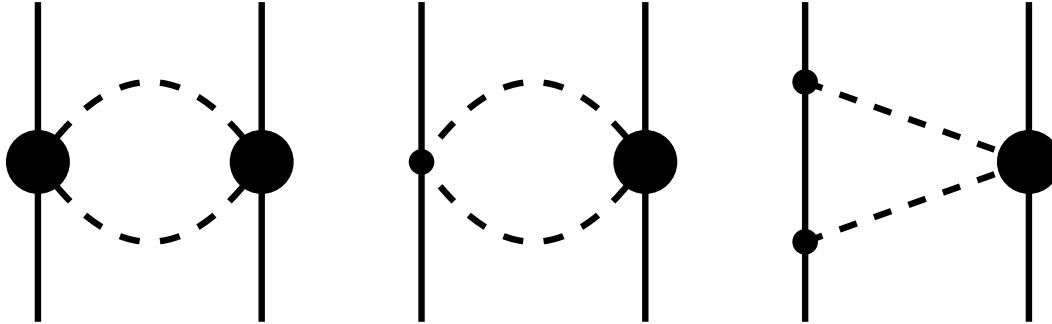


Fig.2: The heavy dot symbolizes the second order chiral $\pi\pi NN$ -contact vertex proportional to the low energy constants $c_{1,2,3,4}$. The 2π -exchange diagrams for which the role of both nucleons is interchanged are not shown.

Furthermore, we like to present here results for another class of new contributions to the NN-potential at order $\mathcal{O}(Q^4)$. This includes the one-loop 2π -exchange diagram with two second order chiral $\pi\pi NN$ -vertices proportional to the low energy constants $c_{1,2,3,4}$ and the first relativistic $1/M$ -corrections to the 2π -exchange diagrams with one such vertex proportional to $c_{1,2,3,4}$. The corresponding graphs are shown in Fig. 2. The first "bubble" or "football" diagram can be straightforwardly evaluated in the heavy baryon formalism and one finds [13],

$$V_C(q) = -\frac{3L(q)}{16\pi^2 f_\pi^4} \left\{ \left[\frac{c_2}{6} w^2 + c_3(2m_\pi^2 + q^2) - 4c_1 m_\pi^2 \right]^2 + \frac{c_2^2}{45} w^4 \right\}, \quad (10)$$

$$W_T(q) = -\frac{1}{q^2} W_S(q) = -\frac{c_4^2}{96\pi^2 f_\pi^4} w^2 L(q), \quad (11)$$

with the frequently occurring loop function,

$$L(q) = \frac{w}{q} \ln \frac{w+q}{2m_\pi}, \quad w = \sqrt{4m_\pi^2 + q^2}. \quad (12)$$

In eqs.(10,11) and in the following we omit purely polynomial terms of the form $\text{const } q^4 + \text{const } q^2 + \text{const}$ in the central NN-amplitudes and $\text{const } q^2 + \text{const}$ in the tensor and spin-orbit NN-amplitudes. The third diagram in Fig. 2 with one $c_{1,2,3,4}$ -vertex starts to contribute at order $\mathcal{O}(Q^3)$ (see section 4 in ref.[5]) and the next higher order contribution at $\mathcal{O}(Q^4)$ arises from the first relativistic $1/M$ -corrections to the vertices and nucleon propagator. In order to be specific we employ here the minimal relativistic second order πN -Lagrangian $\mathcal{L}_{\pi N}^{(2,min)}$ defined in ref.[11]. A convenient way to obtain the $1/M$ -corrections is to use relativistic nucleon propagators and interaction vertices and to perform (in the NN center-of-mass frame) the $1/M$ -expansion inside the pion-loop integral. Consider now the second diagram in Fig. 2 (and its mirror partner). Since the left hand side Tomozawa-Weinberg vertex is of isovector nature only the isovectorial c_4 -vertex can contribute on the right hand side. One finds modulo polynomials,

$$W_{SO}(q) = 2W_T(q) = -\frac{2}{q^2} W_S(q) = -\frac{2}{q^2} W_C(q) = -\frac{c_4}{96\pi^2 M f_\pi^4} w^2 L(q). \quad (13)$$

As a genuine relativistic effect we encounter here a spin-orbit NN-amplitude $W_{SO}(q)$. According to the convention of ref.[5, 6] the spin-orbit amplitudes are accompanied in the NN T-matrix by the (momentum space) spin-orbit operator $i(\vec{\sigma}_1 + \vec{\sigma}_2) \cdot (\vec{q} \times \vec{p})$, where \vec{p} denotes the nucleon

center-of-mass momentum. The c_4 -vertex in the third diagram of Fig. 2 (and its mirror partner) generates further isovector NN-amplitudes,

$$W_T(q) = -\frac{1}{q^2}W_S(q) = \frac{c_4g_A^2}{192\pi^2Mf_\pi^4}(16m_\pi^2 + 7q^2)L(q), \quad (14)$$

$$W_{SO}(q) = -\frac{2}{q^2}W_C(q) = -\frac{c_4g_A^2}{96\pi^2Mf_\pi^4}(8m_\pi^2 + 5q^2)L(q). \quad (15)$$

Finally, the isoscalar NN-amplitudes stem from the isoscalar $c_{1,2,3}$ -vertex in the last diagram of Fig. 2 and they read (modulo polynomials),

$$V_{SO}(q) = \frac{c_2g_A^2}{16\pi^2Mf_\pi^4}w^2L(q), \quad (16)$$

$$V_C(q) = \frac{g_A^2L(q)}{32\pi^2Mf_\pi^4} \left[(c_2 - 6c_3)q^4 + 4(6c_1 + c_2 - 3c_3)q^2m_\pi^2 + 6(c_2 - 2c_3)m_\pi^4 + 24(2c_1 + c_3)m_\pi^6w^{-2} \right]. \quad (17)$$

Note that there are no isoscalar spin-spin and tensor NN-amplitudes $V_{S,T}(q)$. This follows from the fact that to first order in the $1/M$ -expansion the $c_{1,2,3}$ -vertex remains spin-independent. For the sake of completeness we give also the spectral representation of the spin-orbit potential in coordinate space (accompanying the standard spin-orbit operator $-\frac{i}{2}(\vec{\sigma}_1 + \vec{\sigma}_2) \cdot (\vec{r} \times \vec{\nabla})$) which reads,

$$\tilde{V}_{SO}(r) = \frac{1}{\pi^2r^3} \int_{2m_\pi}^{\infty} d\mu \mu e^{-\mu r} (1 + \mu r) \text{Im} V_{SO}(i\mu). \quad (18)$$

With the help of the formula $\text{Im} L(i\mu) = -\pi k/\mu = -(\pi/2\mu)\sqrt{\mu^2 - 4m_\pi^2}$ the numerical evaluation of the coordinate space NN-potentials following from the one-loop results eqs.(10–17) is straightforward.

In summary, we have calculated in this work the chiral 2π -exchange NN-potentials at two-loop order. We find that these two-loop diagrams lead to a sizeable isoscalar central repulsion. Furthermore, we have evaluated here the one-loop 2π -exchange diagram with two second order $c_{1,2,3,4}$ -vertices as well as the first relativistic $1/M$ -correction to the diagrams with one such vertex. The analytical results presented here are in a form such that they can be easily implemented in a $N^3\text{LO}$ calculation of the two-nucleon system or in an empirical analysis of low-energy elastic NN-scattering.

References

- [1] S. Weinberg, *Nucl. Phys.* **B363**, 3 (1991).
- [2] C. Ordóñez, L. Ray and U. van Kolck, *Phys. Rev.* **C53**, 2086 (1996).
- [3] D.B. Kaplan, M.J. Savage and M.B. Wise, *Nucl. Phys.* **B534**, 329 (1998).
- [4] E. Epelbaum, W. Glöckle and Ulf-G. Meißner, *Nucl. Phys.* **A637**, 107 (1998); **A671**, 295 (2000).
- [5] N. Kaiser, R. Brockmann and W. Weise, *Nucl. Phys.* **A625**, 758 (1997).
- [6] N. Kaiser, S. Gerstendörfer and W. Weise, *Nucl. Phys.* **A637**, 395 (1998).
- [7] M.C.M. Rentmeester, R.G.E. Timmermans, J.L. Friar and J.J. de Swart, *Phys. Rev. Lett.* **82**, 4992 (1999).
- [8] R. Machleidt and D. Phillips, private communications.
- [9] N. Kaiser, *Phys. Rev.* **C61** 014003 (2000); **C62** 024001 (2000); **C63** 044010 (2001).
- [10] V. Bernard, N. Kaiser and Ulf-G. Meißner, *Nucl. Phys.* **A615**, 483 (1997).
- [11] N. Fettes, Ulf-G. Meißner and S. Steininger, *Nucl. Phys.* **A640**, 199 (1998).
- [12] M.M. Pavan et al., *Physica Scripta*, **T87** 65 (2000).
- [13] The same result has been independently obtained by E. Epelbaum (unpublished).